

Unusual ferroelectricity induced by the Jahn-Teller effect: A case study on lacunar spinel compounds

Ke Xu^{1,2,3} and H. J. Xiang^{1,3,*}

¹Key Laboratory of Computational Physical Sciences (Ministry of Education), State Key Laboratory of Surface Physics, and Department of Physics, Fudan University, Shanghai 200433, People's Republic of China

²Hubei Key Laboratory of Low Dimensional Optoelectronic Materials and Devices, Hubei University of Arts and Science, Xiangyang, 441053, People's Republic of China

³Collaborative Innovation Center of Advanced Microstructures, Nanjing 210093, People's Republic of China

(Received 15 June 2015; published 28 September 2015)

The Jahn-Teller effect refers to the symmetry-lowering geometrical distortion in a crystal (or nonlinear molecule) due to the presence of a degenerate electronic state. Usually, the Jahn-Teller distortion is not polar. Recently, GaV_4S_8 with a lacunar spinel structure was found to undergo a Jahn-Teller distortion from a cubic to ferroelectric rhombohedral structure at $T_{JT} = 38$ K. Here, we carry out a general group theory analysis to show how and when the Jahn-Teller effect gives rise to ferroelectricity. On the basis of this theory, we find that the ferroelectric Jahn-Teller distortion in GaV_4S_8 is due to the noncentrosymmetric nature of the parent phase and a strong electron-phonon interaction related to two low-energy T_2 phonon modes. Interestingly, GaV_4S_8 is not only ferroelectric, but also ferromagnetic with a magnetic easy axis along the ferroelectric direction. This suggests that GaV_4S_8 is a multiferroic material in which an external electric field may control its magnetization direction. Our study not only explains the Jahn-Teller physics in GaV_4S_8 , but also paves a way for searching and designing different ferroelectrics and multiferroics.

DOI: [10.1103/PhysRevB.92.121112](https://doi.org/10.1103/PhysRevB.92.121112)

PACS number(s): 75.85.+t, 71.20.-b, 71.38.-k, 71.70.Ej

In 1937, Jahn and Teller performed a symmetry analysis to demonstrate that a nonlinear polyatomic molecule with degenerated orbitals is not stable and it will spontaneously distort itself in some way to remove its degeneracy [1]. Later, the Jahn-Teller (JT) effect was found to also take place in solids as a special case of electron-phonon coupling [2]. It turns out that the JT effect is relevant to many exotic phenomena in condensed matter physics. For example, some models have been put forward to understand the role of the JT effect in the high- T_c (T_c means critical temperature) superconductivity in cuprates [3–9]. The JT effect is also a key ingredient for understanding colossal magnetoresistance in manganites [10–13].

Usually, the JT distortion is of a nonpolar nature, i.e., it does not induce ferroelectricity. Perovskite KCuF_3 and LaMnO_3 are two typical examples in which the cooperative JT effect takes place and induces orbital ordering [12–14]. At high temperatures, both KCuF_3 and LaMnO_3 are cubic with the $Pm\bar{3}m$ space group. The low temperature phases of KCuF_3 and LaMnO_3 take the $I4/mcm$ [14,15] and $Pnma$ [10] space groups, respectively. Although their symmetry is lowered by the JT distortion, the centrosymmetry remains intact. The above experimental fact makes most believe that the JT effect could not give rise to proper ferroelectricity. Note that here we focus on the original JT effect, instead of the pseudo-JT effect (or second-order JT effect), which is responsible for the ferroelectricity in many common ferroelectrics such as BaTiO_3 [16,17].

Interestingly, a recent study indicates that the JT distortion in GaV_4S_8 leads to a ferroelectric polarization ($\sim 0.6 \mu\text{C cm}^{-2}$) along the [111] direction [18,19]. GaV_4S_8 belongs to the family of lacunar spinel AM_4X_8 compounds [20–23] ($A =$

Ga and Ge ; $M = \text{V}, \text{Mo}, \text{Nb}$, and Ta ; $X = \text{S}$ and Se), which have attracted enormous research attention since they exhibit abundant physical phenomena, such as a high pressure induced superconducting phase transition [24] and a correlation-driven insulator-to-metal transition [25,26]. At room temperature, GaV_4S_8 takes a high symmetry lacunar spinel structure with T_d symmetry (i.e., noncentrosymmetric and nonpolar). At 42 K, the cooperative JT distortion drives a cubic-to-rhombohedral (C_{3v} symmetry) structural transition. We note that a similar JT distortion induced ferroelectricity was also observed in the lacunar spinel compound GeV_4S_8 [27]. A complete understanding of the JT distortion induced ferroelectricity in lacunar spinel compounds is still missing. The answer to this question is not only relevant to lacunar spinel compounds, but also may lead to other directions for designing and predicting different ferroelectrics and multiferroics.

In this Rapid Communication, we explore the possibility of inducing ferroelectricity through the JT effect. A general group theory analysis is performed to show that the JT effect might induce ferroelectricity if the parent structure belongs to one of ten nonpolar, noncentrosymmetric point groups. By combining group theory analysis and first-principles calculations on the electron-phonon coupling constants, we find that the noncentrosymmetric nature of cubic GaV_4S_8 and the presence of two low-energy T_2 modes with strong electron-phonon coupling are crucial to the occurrence of ferroelectricity induced by the JT distortion. We propose that the magnetic easy axis can be controlled by an external magnetic field in multiferroic $R\bar{3}m$ GaV_4S_8 . Finally, we predict that the JT effect will also induce ferroelectricity in GaMo_4S_8 , and that $R\bar{3}m$ GaMo_4S_8 is a ferromagnetic multiferroic.

Let us assume that a parent high symmetry structure (G_0 space group) with an equilibrium configuration Q_0 has a degenerate electronic ground state, i.e., an n -fold degenerate level of the original electronic Hamiltonian H_0 is partially

*hxiang@fudan.edu.cn

filled. The single particle wave functions of the degenerate states are denoted by ϕ_i ($i = 1, n$). The JT effect results in a lower symmetry nuclear configuration Q , which can be obtained from the high symmetry equilibrium configuration Q_0 by adding a linear combination of phonon normal modes, $Q = Q_0 + \sum_r \eta_r Q_r$ (η_r is the magnitude of the normal mode Q_r). The electronic Hamiltonian of the distorted structure can be expanded as a power series in terms of η_r . For our current purpose, it is adequate to consider the terms up to the linear order,

$$H = H_0 + H' = H_0 + \sum_r \frac{\partial V}{\partial \eta_r} \eta_r, \quad (1)$$

where V is the one-electron crystalline potential. To investigate how the distortion splits the degenerate level, one can adopt the degenerate perturbation theory by diagonalizing the $n \times n$ matrix with the matrix elements defined below:

$$H'_{ij} = \sum_r \eta_r \langle \phi_j | \frac{\partial V}{\partial \eta_r} | \phi_i \rangle. \quad (2)$$

For simplicity, we consider the Γ normal modes and Γ electronic states. In this case, the point group K_0 of the space group G_0 can be used to classify ϕ_i and $\frac{\partial V}{\partial \eta_r}$. Note that $\frac{\partial V}{\partial \eta_r}$ has the same symmetry transformation property as the normal mode Q_r . We assume that ϕ_i and Q_r transform as irreducible representations (IRs) \hat{D}_e and \hat{D}_p , respectively. According to the group theory, only when the product $\phi_j^* \frac{\partial V}{\partial \eta_r} \phi_i$ contains an identical representation, or equivalently, the symmetrical product ($\hat{D}_e^{[2]}$) of \hat{D}_e contains \hat{D}_p , can the integral $\langle \phi_j | \frac{\partial V}{\partial \eta_r} | \phi_i \rangle$ be nonzero. Otherwise, the degenerate electronic states will not split, and the JT distortion will not take place.

If the point group K_0 of the parent structure contains spatial inversion symmetry, one can easily show that the JT effect will not break centrosymmetry. For a point group containing inversion symmetry, the IR is either even (g) or odd (u). The IR for ϕ_i can be even or odd. In any case, the symmetrical product $\hat{D}_e^{[2]}$ only contains even IRs. If the normal mode Q_r has an odd symmetry, $\langle \phi_j | \frac{\partial V}{\partial \eta_r} | \phi_i \rangle$ will be zero. This means that the JT distortion should not contain odd normal modes when the parent structure is centrosymmetric. Thus, we explain why the JT distortion cannot induce ferroelectricity in centrosymmetric systems such as KCuF_3 and LaMnO_3 . The JT distortion was found to induce local electric polarization in DyVO_4 and PrCl_3 because the site symmetry of Dy^{3+} and Pr^{3+} is noncentrosymmetric. However, the overall polarization cancels, resulting in an antiferroelectric structure [28,29]. This is because the point group of the high temperature structures of DyVO_4 and PrCl_3 contains centrosymmetry. Our group theory analysis shows that, instead of a local site symmetry, the overall symmetry of the parent structure should be adopted to predict whether the JT effect can induce ferroelectricity.

As we discussed above, the JT effect cannot induce ferroelectricity if the parent structure is centrosymmetric. If the parent structure itself is polar, the JT effect may give rise to an additional electric polarization. However, the electric polarization may not be switched. Below, we will focus on the case where the parent structure is nonpolar and noncentrosymmetric. Of the 32 crystal point groups, there are 11 nonpolar and noncentrosymmetric point groups, namely,

D_2 , S_4 , D_4 , D_{2d} , D_3 , C_{3h} , D_6 , D_{3h} , T , O , and T_d point groups. Since the D_2 point group does not have any degenerate IRs, there is no JT effect in a parent structure with such a point group symmetry. For each of the other ten point groups, we consider each degenerate IR \hat{D}_e for the electronic states. Then the symmetrical product $\hat{D}_e^{[2]}$ is decomposed into IRs from which the IR \hat{D}_p of the normal mode of the JT distortion is selected. If general, the normal mode of a given IR \hat{D}_p is characterized by its order parameter direction. For each possible normal mode of the IR \hat{D}_p , we determine the point group of the final distorted structure to tell whether the JT effect induces ferroelectricity. All these results are listed in Ref. [30]. In particular, we find that the JT distortion will always induce ferroelectricity when a parent structure with S_4 , D_3 , C_{3h} , or D_{3h} point groups has a degenerate electronic state and the cell size is not enlarged. Therefore, the JT effect may induce ferroelectricity when the point group of the parent structure is nonpolar and noncentrosymmetric. This is one of our main results.

Now we begin to address why the JT effect gives rise to ferroelectricity in GaV_4S_8 . At room temperature, cubic GaV_4S_8 exhibits the $F\bar{4}3m$ space group and the four V atoms occupy the 16e Wyckoff position with the site symmetry C_{3v} , which forms a regular tetrahedral structure [see Fig. 1(a)] and the V-V bond length is about 2.89 Å [Fig. 1(c)]. The band structure and schematic illustration of the energy levels of cubic GaV_4S_8 are shown in Fig. 2. Here, the spin unpolarized state is considered. Our calculations show that there is a narrow partially filled threefold degenerate t_2 band. The fat band analysis shows that this degenerate band is mainly contributed from the 3d orbitals of the V_4 cluster. In GaV_4S_8 , each V ion is in the +3.25 valence state. Thus, there are seven valence electrons per V_4 cluster, among which six electrons fully occupy the low-energy a_1 and e levels [see Fig. 2(b)] and

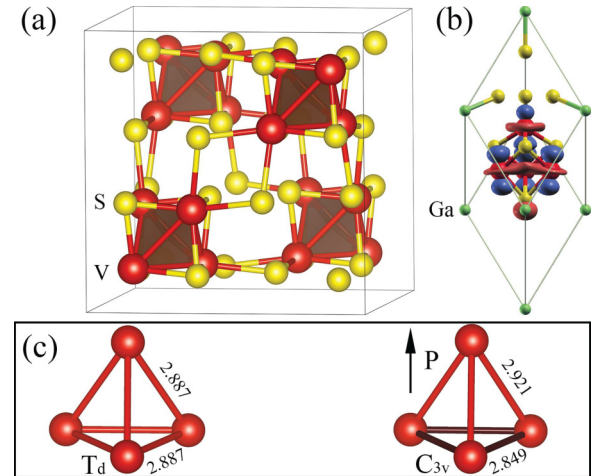


FIG. 1. (Color online) Structure and wave function of lacunar spinel GaV_4S_8 . (a) The conventional cell of GaV_4S_8 with the cubic $F\bar{4}3m$ symmetry. The V_4 tetrahedra are displayed. Ga atoms are not shown for clarity. (b) The isosurface plot of the highest occupied Γ wave function with the a_1 symmetry of the low symmetry $R3m$ structure. (c) The comparison of the V_4 tetrahedron between cubic T_d GaV_4S_8 and rhombohedral C_{3v} GaV_4S_8 . The direction of ferroelectric polarization is also shown in the case of C_{3v} GaV_4S_8 .

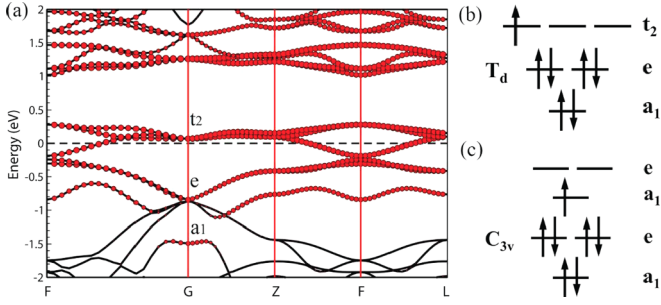


FIG. 2. (Color online) Electronic properties of GaV₄S₈. (a) The band structure of cubic GaV₄S₈ from the spin unpolarized DFT calculation. The Fermi energy is set to zero. Red circles denote the contributions from the 3d orbitals of V atoms. (b), (c) Schematic illustrations of the energy levels related to V₄ clusters in T_d GaV₄S₈ and C_{3v} GaV₄S₈, respectively.

the remaining electron partially fills the threefold degenerate t_2 level [31]. This indicates that GaV₄S₈ is a JT active system.

Since cubic GaV₄S₈ with the noncentrosymmetric T_d point group has a degenerate electronic state on the t_2 level, the JT effect may give rise to ferroelectricity, according to our above group theory analysis. The symmetrical product of t_2 can be decomposed as $t_2^{(2)} = a_1 \oplus e \oplus t_2$. Therefore, the active normal mode can possibly belong to $A_1(\Gamma_1)$, $E(\Gamma_3)$, or $T_2(\Gamma_4)$. Since A_1 is a fully symmetric representation which cannot split the electronic level, this mode is not relevant. We find that the T_2 mode can induce ferroelectricity, while the E mode cannot (see Fig. 3). The group theory can only show that there is a possibility to induce ferroelectricity by the JT effect in GaV₄S₈ since it cannot determine which normal mode (E or T_2) will be active.

In order to determine the exact normal mode in the low temperature GaV₄S₈ structure, we will minimize the total energy with respect to the distortion. Within our simple model, the total energy of the distorted structure contains two parts,

$$E(Q) = E_{\text{strain}}(Q) + E_{\text{JT}}(Q), \quad (3)$$

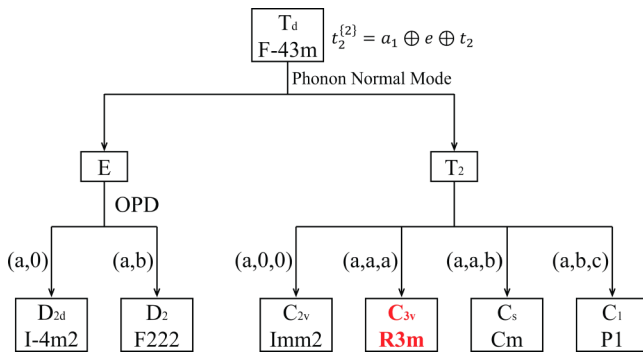


FIG. 3. (Color online) Possible JT distortions in a T_d compound with a partially occupied t_2 electronic level. From the symmetrical product of t_2 , one obtains the JT active irreducible representations (IRs) of phonon normal modes. For each possible phonon IR, the JT active normal mode is characterized by the order parameter direction (OPD). For each normal mode, the symmetry of the resulting distorted structure is denoted. The lacunar spinel GaV₄S₈ takes the ferroelectric C_{3v} $R3m$ structure after the JT distortion.

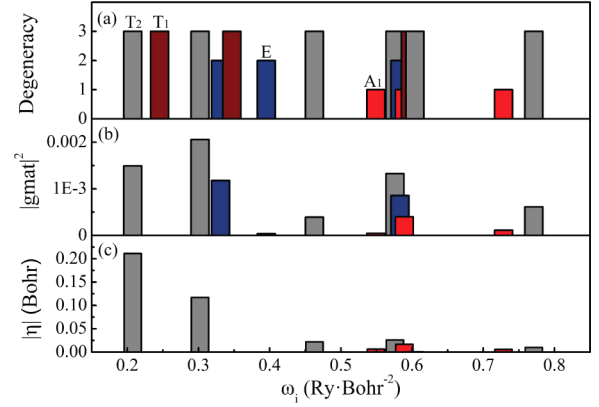


FIG. 4. (Color online) Predicted JT distortion in GaV₄S₈ on the basis of the model including electron-phonon coupling. (a) The frequencies (ω_i is the eigenvalue of the force constant matrix) and the degeneracy of normal modes at Γ . The trivial translational modes are not shown. (b) The amplitude of electron-phonon coupling coefficients, which is defined as $|gmat|^2 = \sum_{i,j,k} |g_{ij}^k|^2$, where g_{ij}^k is the electron-phonon matrix element, and k is the index for the summation over the dimension of the IR of the phonon normal mode. (c) The magnitude of phonon normal modes in the JT distortion. Most of the phonon normal modes have T_2 symmetry. Gray: T_2 mode; wine: T_1 mode; navy: E mode; red: A_1 mode.

where $E_{\text{strain}}(Q)$ is the elastic strain energy cost and $E_{\text{JT}}(Q)$ is the electronic energy gain due to the JT effect. Using the eigenvectors of the force constant matrix (not dynamic matrix) as the normal modes Q_r , the strain energy can be written as $E_{\text{strain}} = \sum_r \omega_r \eta_r^2$, where ω_r is the eigenvalue of the force constant matrix. The electronic energy $E_{\text{JT}}(Q)$ is the sum of eigenvalues of the occupied states, $E_{\text{JT}}(Q) = \sum_{i=1}^n f_i \varepsilon_i(Q)$, where f_i is the Fermi-Dirac distribution and ε_i is the eigenvalue of the electronic states for the distorted nuclear configuration Q . To obtain ε_i , we diagonalize the perturbed Hamiltonian H' with the matrix elements defined in Eq. (2). In practical calculations, the electron-phonon matrix element $g_{ij}^r = \langle \phi_j | \frac{\partial V}{\partial \eta_r} | \phi_i \rangle$ is computed through the density functional perturbation theory. We minimize the total energy with respect to Q (in fact, the magnitude of the normal modes η_r) by combining the Monte Carlo annealing with conjugate gradient local optimization (see Ref. [30]).

Each GaV₄S₈ primitive cell contains one formula unit. So, there are 39 phonon normal modes, which can be classified into three T_1 modes, seven T_2 modes, three E modes, and three A_1 modes [Fig. 4(a)]. In cubic GaV₄S₈, the partially filled degenerate electronic t_2 state is threefold, i.e., $n = 3$. As already mentioned, we consider only Γ normal modes and Γ electronic states. The magnitude of the electron-phonon matrix element is shown in Fig. 4(b). We find that two low frequency T_2 normal modes (at around 0.2 and 0.3 Ry/bohr²) couple strongly to the electronic t_2 state. Note that the lower T_2 mode has the lowest frequency except for the zero-frequency acoustic modes. The lowest frequency E_2 mode (at 0.33 Ry/bohr²) couples more weakly to the electronic t_2 state than the nearby T_2 mode. The electron-phonon matrix elements for the T_1 modes (not shown) are found to be negligible, in agreement with the group theory analysis.

Through minimizing the total energy $E(Q)$, we obtain the distorted structure of GaV_4S_8 . The contribution to the distortion from each normal mode is shown in Fig. 4(c). It can be seen that the two low-energy T_2 modes are dominant with some tiny contribution from other T_2 and A_1 modes. Due to the JT effect, the system distorts according to the T_2 modes with the order parameter direction along (a, a, a) , lowering the symmetry of GaV_4S_8 from T_d to C_{3v} and resulting in ferroelectricity, in agreement with the experimental results. Meanwhile, the original degenerate t_2 electronic state splits into an occupied nondegenerate a_1 level and an unoccupied twofold degenerate e level, as shown in Fig. 2(b). It is interesting to find that there is no contribution to the distortion from the E modes, despite the fact that the electron-phonon coupling related to the E modes is substantial. We perform a test calculation to find that a stronger electron-phonon coupling (e.g., two times stronger) for the E mode results in a different distorted structure with a nonpolar D_{2d} symmetry. It is clear that there is a competition between the two low-energy T_2 modes and E modes in lowering the electronic energy $E_{JT}(Q)$. Because the two T_2 modes are softer and the electron-phonon coupling for the T_2 modes is even stronger than the E modes, the JT effect induces ferroelectricity in GaV_4S_8 .

The way that GaV_4S_8 distorts can be reasoned in terms of the orbital interaction picture. Figure 1(b) shows the Γ wave function (a_1 symmetry) of the highest occupied valence band of the experimental low symmetry $R3m$ GaV_4S_8 structure. The a_1 state is mainly contributed by the d_{z^2} orbitals (here, the local z axis is along the ferroelectric [111] direction) of the four V atoms. We can see that the three d_{z^2} orbitals of the lateral V atoms form a three-center bonding, while the d_{z^2} orbital of the apex V atom interacts with the other d_{z^2} orbitals in an antibonding way. To make the occupied a_1 state more stable, the three lateral V atoms should move towards each other, while the apex V atom should move away from the V triangle. That is exactly what is found experimentally [see Fig. 1(c)]. In the low temperature $R3m$ structure, the distance between the lateral V atoms is 2.85 Å, which is 0.07 Å shorter than that between the apex V atom and the lateral V atoms [Fig. 1(c)].

We now turn to the physical properties of the low temperature rhombohedral phase of GaV_4S_8 . Experiments showed that $R3m$ GaV_4S_8 is a ferromagnetic semiconductor. Our

density functional theory plus Hubbard U calculations confirm that it is semiconducting with an indirect band gap of 0.483 eV [30]. The total magnetic moment for the ferromagnetic state is calculated to be $1 \mu_B/\text{f.u.}$, in agreement with the experimental results [32]. With the Berry phase approach, we find that the electric polarization along the [111] direction is $2.43 \mu\text{C}/\text{cm}^2$, which is larger than the experimentally measured value (about $0.6 \mu\text{C}/\text{cm}^2$). This is reasonable since the band gap of $R3m$ GaV_4S_8 is not large, which may lead to a charge leakage in the measurement. Since $R3m$ GaV_4S_8 is simultaneously ferromagnetic and ferroelectric, it is a multiferroic material, as recently discovered experimentally. We propose that this multiferroic displays an interesting magnetoelectric coupling. Including the spin-orbit coupling effect, our calculations show that $R3m$ GaV_4S_8 displays a magnetic anisotropy with the magnetic easy axis along the ferroelectric [111] direction and an anisotropy energy as large as 5.47 meV. The easy axis behavior is in agreement with the experimental results [18]. This indicates that direction of magnetization is always interlocked with the direction of electric polarization. In a cubic system, there are eight [111] directions. This means that there may exist eight different ferroelectric (FE) domains in the low temperature sample of GaV_4S_8 . If an electric field induces a 109° or 71° switch of the FE polarization, the magnetization easy axis will also rotate by 109° or 71° [30]. This mechanism for the electric field control of magnetism is similar to that proposed in the predicted room temperature multiferroic $\text{Zn}_2\text{FeOsO}_6$ [33]. Lastly, we predict that GaMo_4S_8 is also a multiferroic with similar properties to those of GaV_4S_8 [30].

Note added. Recently, we became aware that Barone *et al.* discussed the possibility of designing multiferroics based on the JT effect [34]. The proposed materials ($\text{Ba}_2\text{VGe}_2\text{O}_7$ and $\text{Ba}_2\text{NiGe}_2\text{O}_7$) were found to have an antiferroelectric ground state.

Work was supported by NSFC (Grant No. 11374056), the Special Funds for Major State Basic Research (Grants No. 2012CB921400 and No. 2015CB921700), Program for Professor of Special Appointment (Eastern Scholar), Fok Ying Tung Education Foundation, FANEDD, and NCET-10-0351. We thank Professor Jianjun Xu for helpful discussions. K.X. was partially supported by NSFC 11404109.

-
- [1] H. A. Jahn and E. Teller, *Proc. R. Soc. London, Ser. A* **161**, 220 (1937).
 [2] M. C. M. O'Brien and C. C. Chancey, *Am. J. Phys.* **61**, 688 (1993).
 [3] S. Margadonna and G. Karotsis, *J. Mater. Chem.* **17**, 2013 (2007).
 [4] J. A. Alonso, M. J. Martínez-Lope, M. T. Casais, and M. T. Fernández-Díaz, *Inorg. Chem.* **39**, 917 (2000).
 [5] H. Sawada, Y. Morikawa, K. Terakura, and N. Hamada, *Phys. Rev. B* **56**, 12154 (1997).
 [6] N. Binggeli and M. Altarelli, *Phys. Rev. B* **70**, 085117 (2004).
 [7] Yu. B. Gaididei and V. M. Loktev, *Phys. Status Solidi B* **147**, 307 (1988).
 [8] W. Weber, A. L. Shelankov, and X. Zotos, *Physica C* **162**, 307 (1989).
 [9] D. V. Fil, O. I. Tokar, A. L. Shelankov, and W. Weber, *Phys. Rev. B* **45**, 5633 (1992).
 [10] I. Loa, P. Adler, A. Grzechnik, K. Syassen, U. Schwarz, M. Hanfland, G. Kh. Rozenberg, P. Gorodetsky, and M. P. Pasternak, *Phys. Rev. Lett.* **87**, 125501 (2001).
 [11] J. Deisenhofer, I. Leonov, M. V. Eremin, Ch. Kant, P. Ghigna, F. Mayr, V. V. Iglamov, V. I. Anisimov, and D. van der Marel, *Phys. Rev. Lett.* **101**, 157406 (2008).
 [12] E. Pavarini and E. Koch, *Phys. Rev. Lett.* **104**, 086402 (2010).
 [13] M. Baldini, V. V. Struzhkin, A. F. Goncharov, P. Postorino, and W. L. Mao, *Phys. Rev. Lett.* **106**, 066402 (2011).

- [14] J. S. Zhou, J. A. Alonso, J. T. Han, M. T. Fernández-Díaz, J. G. Cheng, and J. B. Goodenough, *J. Fluorine Chem.* **132**, 1117 (2001).
- [15] E. Pavarini, E. Koch, and A. I. Lichtenstein, *Phys. Rev. Lett.* **101**, 266405 (2008).
- [16] A. J. Millis, *Nature (London)* **392**, 147 (1998).
- [17] J. M. Rondinelli, A. S. Eidelson, and N. A. Spaldin, *Phys. Rev. B* **79**, 205119 (2009); P. Garcia-Fernandez and I. B. Bersuker, *Phys. Rev. Lett.* **106**, 246406 (2011).
- [18] E. Ruff, S. Widmann, P. Lunkenheimer, V. Tsurkan, S. Bordács, I. Kézsmárki, and A. Loidl, [arXiv:1504.00309](https://arxiv.org/abs/1504.00309).
- [19] I. Kézsmárki, S. Bordács, P. Milde, E. Neuber, L. M. Eng, J. S. White, H. M. Rønnow, C. D. Dewhurst, M. Mochizuki, K. Yanai, H. Nakamura, D. Ehlers, V. Tsurkan, and A. Loidl, *Nature Mater.* (2015).
- [20] D. Brasen, J. M. Vandenberg, M. Robbins, R. H. Willens, W. A. Reed, R. C. Sherwood, and X. J. Pinder, *J. Solid State Chem.* **13**, 298 (1975).
- [21] H. Haeuseler, S. Reil, and E. Elitok, *Int. J. Inorg. Mater.* **3**, 409 (2001).
- [22] D. Johrendt, *Z. Anorg. Allg. Chem.* **624**, 952 (1998).
- [23] C. Vaju, J. Martial, E. Janod, B. Corraze, V. Fernandez, and L. Cario, *Chem. Mater.* **20**, 2382 (2008).
- [24] M. M. Abd-Elmeguid, B. Ni, D. I. Khomskii, R. Pocha, D. Johrendt, X. Wang, and K. Syassen, *Phys. Rev. Lett.* **93**, 126403 (2004).
- [25] A. Camjayi, C. Acha, R. Weht, M. G. Rodríguez, B. Corraze, E. Janod, L. Cario, and M. J. Rozenberg, *Phys. Rev. Lett.* **113**, 086404 (2014).
- [26] V. Ta Phuoc, C. Vaju, B. Corraze, R. Sopracase, A. Perucchi, C. Marini, P. Postorino, M. Chligui, S. Lupi, E. Janod, and L. Cario, *Phys. Rev. Lett.* **110**, 037401 (2013).
- [27] K. Singh, C. Simon, E. Cannuccia, M.-B. Lepetit, B. Corraze, E. Janod, and L. Cario, *Phys. Rev. Lett.* **113**, 137602 (2014).
- [28] J. P. Harrison, J. P. Hessler, and D. R. Taylor, *Phys. Rev. B* **14**, 2979 (1976).
- [29] K. Kishimoto, T. Ishikura, H. Nakamura, Y. Wakabayashi, and T. Kimura, *Phys. Rev. B* **82**, 012103 (2010).
- [30] See Supplemental Material at <http://link.aps.org/supplemental/10.1103/PhysRevB.92.121112> for computational details, results from the group theory analysis, band structure, and the magneto-electric coupling of the $R3m$ GaV₄S₈, and the JT effect induced ferroelectricity in GaMo₄S₈, which includes Refs. [35–45].
- [31] R. Pocha, D. Johrendt, and R. Pöttgen, *Chem. Mater.* **12**, 2882 (2000).
- [32] H. Müller, W. Kockelmann, and D. Johrendt, *Chem. Mater.* **18**, 2174 (2006).
- [33] P. S. Wang, W. Ren, L. Bellaiche, and H. J. Xiang, *Phys. Rev. Lett.* **114**, 147204 (2015).
- [34] P. Barone, K. Yamauchi, and S. Picozzi, *Phys. Rev. B* **92**, 014116 (2015).
- [35] P. Hohenberg and W. Kohn, *Phys. Rev.* **136**, B864 (1964).
- [36] P. E. Blöchl, *Phys. Rev. B* **50**, 17953 (1994).
- [37] G. Kresse and J. Hafner, *Phys. Rev. B* **47**, 558 (1993).
- [38] G. Kresse and J. Furthmüller, *Comput. Mater. Sci.* **6**, 15 (1996).
- [39] J. P. Perdew, K. Burke, and M. Ernzerhof, *Phys. Rev. Lett.* **77**, 3865 (1996).
- [40] V. I. Anisimov, F. Aryasetiawan, and A. I. Lichtenstein, *J. Phys.: Condens. Matter* **9**, 767 (1997).
- [41] H. J. Monkhorst and J. D. Pack, *Phys. Rev. B* **13**, 5188 (1976).
- [42] R. D. King-Smith and D. Vanderbilt, *Phys. Rev. B* **47**, 1651(R) (1993).
- [43] S. Y. Savrasov, D. Y. Savrasov, and O. K. Andersen, *Phys. Rev. Lett.* **72**, 372 (1994).
- [44] P. Giannozzi, S. Baroni, N. Bonini, M. Calandra, R. Car, C. Cavazzoni, D. Ceresoli, G. L. Chiarotti, M. Cococcioni, I. Dabo, A. Dal Corso, S. de Gironcoli, S. Fabris, G. Fratesi, R. Gebauer, U. Gerstmann, C. Gougoussis, A. Kokalj, M. Lazzeri, L. Martin-Samos, N. Marzari, F. Maur, R. Mazzarello, S. Paolini, A. Pasquarello, L. Paulatto, C. Sbraccia, S. Scandolo, G. Sclauzero, A. P. Seitsonen, A. Smogunov, P. Umari, and R. M. Wentzcovitch, *J. Phys.: Condens. Matter* **21**, 395502 (2009).
- [45] H. Stokes, D. Hatch, and B. Campbell, ISOTROPY Software Suite, 2007, <http://stokes.byu.edu/iso/isotropy.php>.